Very Short-Dated Options Pricing

Author:
Prachin Mukesh Patel

Supervisor:
Prof. Laura Ballotta

The Project is submitted as part of the requirements
for the award of the MSc in Financial Mathematics
at the

Bayes Business School (formerly Cass)
City St. George's, University of London

September, 2024

Abstract

This research analyzes which advanced stochastic model best captures the dynamics of very short-term maturity options, focusing on zero days-to-expiry (0DTE) and one day-to-expiry (1DTE) options, with a particular emphasis on the Lévy process and stochastic volatility models. Given the high volatility and sensitivity of these options to new information, it suggests that jump models, particularly those based on the Lévy process with diffusion like Normal Inverse Gaussian (NIG), would better fit market data due to their ability to control higher-order moments. Using S&P 500 options data, the study involves model calibration, out-of-sample analysis, and evaluation of implied density. The results confirm that the Lévy jump diffusion models outperform other models in both fit and predictive accuracy, demonstrating their suitability for pricing very short-term maturity options.

Keywords: Zero days-to-expiry options (0DTEs), Lévy process, stochastic volatilty

1 Introduction

The Black-Scholes model, introduced in 1973 by Fischer Black and Myron Scholes, has been foundational in the field of financial mathematics, providing a theoretical framework for pricing European options. The model's elegant formula for calculating the price of options under the assumption of constant volatility and a log-normal distribution of stock prices revolutionised the trading of derivatives (Black Scholes 1973).

Despite its widespread adoption, the Black-Scholes model exhibits significant limitations, particularly when applied to options with very short maturities, such as zero days-to-expiry (0DTE) options. The assumptions of constant volatility and continuous trading are particularly problematic for 0DTE options, where market dynamics can change rapidly due to immediate events and announcements. These options are especially sensitive to the gamma factor, which measures the rate of change in delta and can lead to substantial hedging challenges as the expiry approaches (Gatheral 2011).

The trading of 0DTEs has seen a significant rise in recent years, reflecting a growing interest among investors and financial institutions. This growth in trading volume is driven by the appeal of capitalising on very short-term market movements, often linked to macroeconomic announcements or other market events (Bandi et al. 2023). The primary objective of this research is to develop and evaluate advanced models capable of accurately pricing short-term options, with a focus on 1 DTE options due to data availability constraints. While the initial aim was to study 0DTE options, inconsistencies in the available data led us to focus on 1 DTE options. However, the methodologies and findings presented here can be readily extended to 0DTE options in future work.

The significance of 0DTE options in modern financial markets is evident from their trading volumes and market share. As of recent years, daily transaction volumes in 0DTE SPX options account for over 43% of the overall daily options volume, equating to a daily notional dollar volume around $1 trillion according to J.P. Morgan Chase's estimates (Bandi et al. 2023). This trend is not limited to the US market; for instance, Deutsche Boerse has introduced 0DTE options on the Euro Stoxx 50 index due to rising institutional demand for short-term hedging instruments (Bandi et al. 2023).

Applications of 0DTE and very short-term options are diverse and impactful, providing significant benefits for various types of investors, including large institutions, mid-size hedge funds, and small retail traders. These options are used for strategies such as hedging macroeconomic event risks, implementing yield-generating programs, and trading tactically around events like Federal Reserve meetings. The ability to quickly respond to market changes makes 0DTE options a valuable tool in the financial services industry (Bandi et al. 2023). On days with significant announcements, such as Federal Open Market Committee (FOMC) meetings, there is often no premium decay before the announcement, followed by rapid declines and increased trading volumes post-announcement (CBOE 2023).

SPX 0DTE volume growth has been remarkable, with a systematic approach being adopted by most traders. Over 95% of the customer opening volume in SPX 0DTE options has limited downside profile, significantly reducing the risk of severe losses (CBOE 2023). Additionally, the robust on-screen liquidity and lower trading costs associated with SPX options make them a preferred vehicle for many investors. The average bid/ask spread in SPX options expiring within one week has trended down to only $0.18, which is less than half a basis point of the index level (CBOE 2023).

Furthermore, 0DTE options have become a focus for regulatory attention due to

their potential systemic risks. The rapid growth and high volume of trades necessitate robust risk management frameworks to mitigate the potential for market disruptions (Bandi et al. 2023). However, pricing 0DTE options presents unique challenges. The short maturity of these options means their gamma is particularly high, especially for at-the-money positions, which can lead to significant hedging difficulties and potential market instability (Bandi et al. 2023). The high sensitivity to underlying price movements requires precise and responsive pricing models.

Currently, there is limited literature on the application of Lévy processes and stochastic volatility models specifically for 0DTE or very short-term options. These mathematical frameworks are potentially well-suited for modelling the erratic price movements and heavy tails typical of very short-term instruments. In this study, we focus on several prominent models in these categories, including the Variance Gamma (VG) model by Madan et al. (1998), the Normal inverse Gaussian (NIG) model by Barndorff-Nielsen (1997), the CGMY model by Carr et al. (2002), the Heston by Heston (1993) and Two-factor Heston stochastic volatility model by Christoffersen et al. (2009). For the Lévy processes the study considers both the types of models that is the pure jump processes and the models with diffusion incorporated. This gap in the literature underscores the need for this research, which aims to explore advanced models capable of capturing the complex dynamics of very short-term options pricing and how improvements can be made further.

Among the evaluated models, the NIG model with the diffusion component demonstrated the best performance in terms of calibration to the implied volatility smile for both in-sample and out-of-sample testing. In contrast, models such as the pure jump VG model and the Two-Heston Model provided the best fit for the implied density relative to market data. Additionally, models incorporating Lévy processes with diffusion outperformed stochastic volatility models. This finding suggests that integrating a jump diffusion model with stochastic volatility could potentially enhance performance in future research. Specifically, models like the Bates (1996) model are expected to significantly improve performance across various aspects and characteristics of options.

This research begins by establishing the theoretical foundation through a careful discussion of the models and numerical schemes that underpin the study, as detailed in Section 2. The methodology is then outlined in Section 3, focusing on the processes of calibration, out-of-sample testing, and implied density estimation that are central to the research approach. Following this, the results of the experimental analysis are presented in Section 4, with a detailed examination of the findings. The paper concludes in Section 5 by bringing together these insights, offering a summary of the contributions and suggesting potential directions for future research.

2 Overview of the models

This chapter provides an overview of the various models and methods used in the pricing of options, with a particular focus on stochastic volatility models and Lévy processes. The discussion primarily addresses the advantages, limitations, and applications of these theoretical frameworks, especially in the context of short maturity options.

In option pricing, the characteristic function enables the problem to be restructured by shifting the focus from time-based variables to a different set of variables. This transformation simplifies the computation of option prices, especially when dealing with complex

models like those involving stochastic volatility or jumps. By applying Fourier transform techniques, the characteristic function enables the calculation of option prices without requiring explicit solutions for the probability density function of the underlying asset's price. This approach not only enhances computational efficiency but also improves accuracy.

2.1 Heston Stochastic Volatility Model

The Heston model, introduced by Heston (1993), is a prominent stochastic volatility model. It assumes that volatility follows a mean-reverting square root process and the model is defined by the following system of stochastic differential equations

$$\begin{aligned} dS_t &= rS_t\,dt + \sqrt{v_t}S_t\,dW_t, \quad \mu \in \mathbb{R}, \\ dv_t &= \kappa(\theta - v_t)\,dt + \eta\sqrt{v_t}\,dZ_t, \\ [W, Z]_t &= \rho t, \quad \rho \in (-1, 1). \end{aligned} \tag{1}$$

where S_t represents the price of the underlying asset, v_t the variance of the asset price, r the drift rate of the asset price under the real world measure, κ the rate of mean reversion of variance, θ the long-term mean variance, η the volatility of variance (volatility of volatility), and W_t and Z_t are two Wiener processes with a correlation ρ.

The Heston model is classified as a stochastic volatility model because it allows the volatility of the underlying asset to be random and to evolve over time according to its own stochastic process. This feature contrasts with the constant volatility assumption in the Black-Scholes model, enabling the Heston model to capture the dynamic nature of market volatility.

One of the key issues the Heston model addresses is the inability of the Black-Scholes model to explain observed market phenomena such as the volatility smile. The Black-Scholes model assumes constant volatility, which often leads to pricing biases, especially for options far from the money. While the volatility smile can be captured by Lévy processes, the term structure of implied volatility cannot be captured by processes with independent and stationary increments. By incorporating stochastic volatility, the Heston model provides a more accurate fit to market data, particularly in explaining return skewness and strike-price biases that are prevalent in real-world financial markets (Heston 1993).

However, the implementation of the Heston model is not without challenges. One notable issue is "The Little Heston Trap," a problem identified by Albrecher et al. (2006). This trap refers to numerical instabilities that can arise when using certain formulations of the characteristic function in the Heston model. Specifically, there are two common specifications of the characteristic function, each being a solution to a Riccati equation. For some parameter choices and long maturities, one of these specifications can lead to instabilities due to branch cuts in the complex plane. The alternative specification avoids these issues, making it crucial to choose the correct formulation to ensure numerical stability. The alternate specification of the characteristic function of the Heston model is given by

$$\phi(u; t) = e^{iu(\ln S_0 + rt) + A(t) + B(t)v_0} \tag{2}$$

with

$$\begin{aligned} A(t) &= \frac{\kappa\theta}{\eta^2}\left((\kappa^M - d)t - 2\ln\left(\frac{1-ge^{-dt}}{1-g}\right)\right) \\ B(t) &= \frac{\kappa^M - d}{\eta^2}\frac{1-e^{-dt}}{1-ge^{-dt}} \\ d &= \sqrt{(\kappa^M)^2 + \eta^2(iu+u^2)} \\ g &= \frac{\kappa^M - d}{\kappa^M + d} \\ \kappa^M &= \kappa - iu\rho \end{aligned} \tag{3}$$

where v_0 is the initial variance.

Despite its robustness and widespread use in financial modelling, the Heston model encounters significant challenges, particularly in the accurate pricing of short-maturity options. One of the primary limitations of the Heston model is its assumption of continuous volatility paths, which contrasts with the observed behavior in real financial markets. Volatility in financial markets often exhibits sudden spikes, a phenomenon known as volatility clustering, especially during periods of market stress or economic uncertainty. These abrupt changes are not adequately captured by the Heston model's continuous diffusion process, leading to potential inaccuracies in pricing options, especially those with short maturities where such sudden volatility shifts can have a pronounced impact.

Moreover, the Heston model does not account for jumps in asset prices, which are common in financial markets. Short-term market events, such as earnings announcements, geopolitical developments, or macroeconomic data releases, can cause sudden and substantial movements in asset prices. The absence of a mechanism to incorporate these jumps means that the Heston model may underestimate the prices of short-maturity options, as it fails to reflect the additional risk associated with these sudden movements.

2.2 Two-Factor Heston Model

Building upon the limitations of the one-factor Heston model, the two-factor Heston model, proposed by Christoffersen et al. (2009), offers a more sophisticated approach to capturing the complexities of market behavior, particularly in relation to the volatility smile and smirk observed in option prices. The one-factor model's assumption of a single source of volatility risk falls short in accurately reflecting the multifaceted nature of market volatility, which is crucial for effectively pricing derivatives, especially short-maturity options. The rigidity of the one-factor model is further highlighted by its inability to allow for different rates of mean reversion for distinct components of volatility.

The two-factor Heston model addresses these shortcomings by introducing two independent variance processes, $V_{1,t}$ and $V_{2,t}$, each governed by its own set of parameters. The model is specified as

$$\begin{aligned} dS_t &= rS_t\,dt + \sqrt{V_{1,t}}S_t\,dZ_{1,t} + \sqrt{V_{2,t}}S_t\,dZ_{2,t}, \\ dV_{1,t} &= \kappa_1(\theta_1 - V_{1,t})\,dt + \eta_1\sqrt{V_{1,t}}\,dZ_{3,t}, \\ dV_{2,t} &= \kappa_2(\theta_2 - V_{2,t})\,dt + \eta_2\sqrt{V_{2,t}}\,dZ_{4,t}. \end{aligned} \tag{4}$$

In this formulation, r represents the risk-free interest rate, while θ_1 and θ_2 denote the long-term average levels of the variance processes $V_{1,t}$ and $V_{2,t}$, respectively. The parameters κ_1 and κ_2 describe the mean reversion speeds of these variances, and η_1 and η_2 capture the

volatilities of these variance processes. The innovation terms $Z_{1,t}$ and $Z_{2,t}$ are uncorrelated with each other, providing independent sources of randomness in the asset price dynamics. Specifically, $Z_{1,t}$ is correlated with $Z_{3,t}$ by ρ_1, and $Z_{2,t}$ is correlated with $Z_{4,t}$ by ρ_2, enabling each variance component to have its own correlation structure with the asset returns.

The introduction of these two independent variance processes also addresses the issue of constant correlation in the one-factor model. In real markets, the correlation between asset prices and their volatility is often time-varying, influenced by a range of factors including market sentiment, macroeconomic conditions, and specific news events. The two-factor Heston model, with its distinct correlation parameters ρ_1 and ρ_2, offers a more realistic and flexible framework for capturing these dynamics, thereby improving the model's accuracy in pricing options.

As a result of these modifications, the characteristic function of the two-factor Heston model differs from that of the single Heston model, as it must account for the contributions of both variance processes. The characteristic function for the two-factor Heston model is defined as:

$$\phi(u;\tau) = e^{iu(\ln S + r\tau) + A(\tau) + B_j(\tau)v_{0_j}}, \tag{5}$$

where the functions $A(\tau)$ and $B_j(\tau)$ are now given by:

$$\begin{aligned} A(\tau) &= \sum_{j=1}^{2} \frac{\kappa_j \theta_j}{\sigma_j^2} \left[\left(\kappa_j^m - d_j\right)\tau - 2\ln\left(\frac{1 - G_j e^{-d_j\tau}}{1 - G_j}\right)\right], \\ B_j(\tau) &= \frac{\left(\kappa_j^m - d_j\right)\left(1 - e^{-d_j\tau}\right)}{\sigma_j^2\left(1 - G_j e^{-d_j\tau}\right)}, \end{aligned} \tag{6}$$

with:

$$\begin{aligned} d_j &= \sqrt{\left(\kappa_j^m\right)^2 + \sigma_j^2\left(u^2 + iu\right)}, \\ G_j &= \frac{\kappa_j^m - d_j}{\kappa_j^m + d_j}, \\ \kappa_j^m &= \kappa_j - iu\rho_j\sigma_j, \quad \text{for } j = 1, 2. \end{aligned} \tag{7}$$

One observes from Christoffersen et al. (2009) that the two-factor Heston model demonstrates substantial improvements over the one-factor model, especially for short-maturity options that are not at-the-money. However, the accuracy of the model comes at the cost of higher complexity that lacks parsimony. Richly parameterised models like the two-factor model often perform well in-sample but can struggle out-of-sample due to overfitting. Additionally, the calibration process becomes more challenging due to the increased number of parameters, making it difficult to find stable and reliable estimates.

Due to the key observations mentioned above, this paper hypothesizes that Lévy models will yield superior results compared to both the one-factor and two-factor Heston models. The rationale behind this hypothesis lies in the inherent parsimony of Lévy models, which allows them to effectively capture the significant characteristics and dynamics of 0DTE option prices. This advantage arises from the increased control over higher-order moments, enabling Lévy models to produce flexible distributions that better accommodate the complexities of financial data. It is expected that this flexibility will result in a more robust fit across different market conditions, reducing the risk of overfitting and improving out-of-sample performance.

However, it is important to note that Lévy processes can introduce discontinuities, which are not ideal for modelling short maturity options. To address these challenges, various techniques have been proposed, including smoothing methods, filtering, numerical approaches, and regularization. These solutions have been extensively discussed in previous literature and offer practical ways to enhance the performance of Lévy models.

2.3 Lévy and Sato Processes

Building on the limitations of the Heston models, including the two-factor extension, several alternative models have been proposed. Lévy processes are advantageous because they incorporate jumps in the asset price dynamics, addressing the shortcomings of the Heston model in capturing sudden market movements and volatility clustering. Furthermore, Lévy processes offer the ability to control higher-order moments such as skewness and kurtosis, which is particularly valuable for modelling and pricing short-maturity options. By allowing for more accurate and realistic distributions of asset returns, Lévy models provide a powerful framework for capturing the nuanced behaviors observed in financial markets. This flexibility is especially beneficial for short-maturity options, where traditional models often fall short.

Lévy processes are a class of stochastic processes with stationary and independent increments. Their significance in financial modelling lies in their ability to capture the empirical features of asset returns, such as heavy tails and skewness, which classical models based on Brownian motion fail to describe adequately. The key result for Lévy processes is their characteristic function, which has an exponential form described by the Lévy-Khintchine representation

$$\mathbb{E}[e^{iuX_t}] = e^{t\psi(u)}, \tag{8}$$

where $\psi(u)$ is the characteristic exponent. The Lévy-Khintchine representation in its entirety is given by

$$\psi(u) = i\gamma u - \frac{1}{2}\sigma^2 u^2 + \int_{\mathbb{R}} \left(e^{iux} - 1 - iux\mathbf{1}_{|x|<1}\right) \nu(dx), \tag{9}$$

where $\gamma \in \mathbb{R}$ is the drift parameter, $\sigma \geq 0$ is the diffusion coefficient of the Brownian motion, and ν is the Lévy measure, satisfying

$$\int_{\mathbb{R}} (1 \wedge x^2)\nu(dx) < \infty. \tag{10}$$

This representation highlights the infinite divisibility of Lévy processes. The Lévy measure $\nu(dx)$ is crucial in describing the jump structure of the process. It determines the intensity and size distribution of the jumps. To further understand this, we introduce the concept of Lévy density. The Lévy measure can often be represented in terms of a density function $\nu(x)$ with respect to the Lebesgue measure, particularly when the jumps are not concentrated on a discrete set. This Lévy density $\nu(x)$ provides a more intuitive understanding of the frequency and magnitude of the jumps.

The general form of a Lévy process X_t can be used to express the stock price at time t as follows

$$S_t = S_0 e^{(r-\psi(-i))t+X_t}, \tag{11}$$

where $\psi(-i)$ is the characteristic exponent evaluated at $-i$ and X_t can be specified as the Variance Gamma (VG), Normal Inverse Gaussian (NIG), or CGMY process, each capturing different aspects of market behaviour.

For a detailed exposition of Lévy processes and their applications in finance, refer to Tankov (2003). An extension to the Lévy processes is the Sato process which introduces inhomogeneous increments. Specifically, a Sato process is derived from a Lévy process whose law at unit time is self-decomposable, allowing for the scaling of the marginal laws to model various timescales. Sato processes primarily affect the characteristic functions by introducing time-dependency. This adjustment allows Sato processes to better fit the observed volatility surfaces and capture the dynamics of financial instruments over time. This enhancement is particularly useful for pricing structured products and long-dated options, where traditional Lévy processes may fall short (Eberlein and Madan 2007).

Mathematically, a Sato process X_t is defined by its self-similarity property

$$X_t \stackrel{d}{=} t^H X_1 \tag{12}$$

where $\stackrel{d}{=}$ denotes equality in distribution, and $H > 0$ is the self-similarity index. The characteristic function of a Sato process takes the form

$$\mathbb{E}[e^{iuX_t}] = e^{\psi(t^H u)} \tag{13}$$

where $\psi(t^H u)$ is the characteristic exponent of the process at $t = 1$. This structure allows for more flexible modelling of the term structure of returns compared to standard Lévy processes. However, the focus of this paper is to examine the applications of Lévy processes, specifically illustrating the characteristic function of versions that include diffusion, as it is easier to revert to the pure jump version from this form. The models will still be referred to by their original acronyms, but a distinction between the two versions will be made in Section 4. For example, VG refers to the Variance Gamma model, while VGB denotes the Variance Gamma model with Brownian motion.

2.4 Variance Gamma Model

The VG process is a three-parameter Lévy process that extends the classical Brownian motion by incorporating jumps. This model was introduced to better capture the skewness (asymmetry) and leptokurtosis (heavy tails) observed in financial return distributions, which traditional models like Black-Scholes fail to account for adequately. The VG process models the log-returns of asset prices more accurately by allowing for jumps, making it particularly suitable for options pricing (Madan et al. 1998).

The VG process $X(t; \eta, \beta\theta)$ can be described as follows

$$X(t; \eta, \beta, \theta) = \theta\Gamma(t; 1, \beta) + \eta W(\Gamma(t; 1, \beta)) + \sigma B_t \tag{14}$$

where $\Gamma(t; 1, \beta)$ is a gamma process with mean t/k and variance $\beta = 1/k$ and $W(\Gamma(t; 1, \beta))$ is the Brownian Motion with a gamma clock assuming independence between them. σ is the volatilty of the Brownian motion B_t which is independent of the Brownian motion $W(\Gamma(t; 1, \beta))$. β allows for the hold over the excess kurtosis with regards to the normal distribution. Here, η represents the volatility of the Brownian motion and is strictly positive ($\eta > 0$). The parameter k is the inverse of the mean rate and variance rate of the gamma process, and it must be non-zero ($k \neq 0$). The parameter θ is the drift

parameter, which controls the degree of skewness of the distribution (Madan et al. 1998). The characteristic function $\phi_X(u;t)$ of the VG process $X(t;\eta,\beta,\theta)$ is given by

$$\phi_X(u;t) = \left(\frac{1}{1 - i\theta\beta u + \frac{1}{2}\eta^2\beta u^2}\right)^{\frac{t}{\beta}} \tag{15}$$

The VG asset price process is described by the following equation

$$S_t = S_0 e^{X_{t,VG}} \tag{16}$$

where $X_{t,VG} = \mu t + X(t;\eta,\beta,\theta)$, and $\mu = r + \omega$ is the drift of the logarithmic asset price (Oosterlee and Grzelak 2019). The characteristic exponent is now updated to

$$\varphi_{VG}(u,t) = \mathbb{E}\left[e^{iuX_{t,VG}}\right] = e^{iu(\mu - \frac{1}{2}\sigma^2)t} e^{-\frac{1}{2}\sigma^2 u^2 t}\left(1 - i\beta\theta u + \frac{1}{2}\beta\eta^2 u^2\right)^{-\frac{t}{\beta}} \tag{17}$$

The characteristic function is modified to accommodate the VG drift adjustment to ensure that the discounted process $e^{-rt}S_t$ is a martingale under the risk-neutral measure. This is achieved by including the drift adjustment term ω given by

$$\omega = \frac{1}{\beta}\log\left(1 - \beta\theta - \frac{1}{2}\beta\eta^2\right) \tag{18}$$

where θ and $\eta^2/2$ are chosen such that $\theta + \eta^2/2 < 1/\beta$ (Oosterlee and Grzelak 2019).

2.5 Normal Inverse Gaussian Model

Looking at another Lévy process of interest, the NIG process is highly relevant to finance because it provides a more accurate representation of asset return distributions. The NIG process is a variance-mean mixture of a normal distribution with an inverse Gaussian distribution as the mixing distribution. This formulation allows for greater flexibility and precision in modelling the probabilistic behaviour of financial returns, which is crucial for pricing derivatives (Barndorff-Nielsen 1997).

The NIG process $X(t;\alpha,\beta,\delta,\sigma)$ is defined by its construction through a normal distribution and an inverse Gaussian distribution. The process can be represented as follows

$$X(t;\alpha,\beta,\delta,\sigma) = \beta\Gamma(t;\delta) + \sigma W(\Gamma(t;\delta)) \tag{19}$$

where $\Gamma(t;\delta)$ is a inverse Gaussain (IG) process with shape parameter t and scale parameter δ, and $W(\Gamma(t;\delta))$ represents Brownian motion evaluated at the IG process. The parameter α denotes the tail heaviness (i.e. steepness of the density) and must be positive ($\alpha > 0$), while β represents the asymmetry parameter and must satisfy $|\beta| < \alpha$. The scale parameter δ is strictly positive ($\delta > 0$), and μ is the location parameter. The characteristic function $\phi_X(u;t)$ of the NIG process $X(t;\alpha,\beta,\delta)$ is given by

$$\phi_X(u;t) = \exp\left(\delta t\left(\sqrt{\alpha^2 - \beta^2} - \sqrt{\alpha^2 - (\beta + iu)^2}\right) - \frac{1}{2}\sigma^2 u^2 t\right) \tag{20}$$

This characteristic function incorporates all four parameters (α, β, δ, μ) and highlights the flexibility of the NIG process in modelling the distribution of returns. It provides a tractable way to compute option prices and other financial derivatives by leveraging

Fourier transform techniques (Barndorff-Nielsen 1997). The NIG asset price process is described by the following equation

$$S_t = S_0 e^{X_{t,NIG}} \tag{21}$$

where $X_{t,NIG}$ is the NIG log-asset price process. The drift correction term which leads to the process being a martingale under Equivalent Martingale Measure (EMM) is given by (Oosterlee and Grzelak 2019)

$$\omega = \delta \left(\sqrt{\alpha^2 - (\beta+1)^2} - \sqrt{\alpha^2 - \beta^2} \right) \tag{22}$$

thus the characteristic exponent becomes

$$\varphi_{NIG}(u,t) = \mathbb{E}\left[e^{iuX_{t,NIG}}\right] = e^{iu(r+\omega-\frac{1}{2}\sigma^2)t}\phi_X(u;t) \tag{23}$$

2.6 CGMY Model

Examining a tempered stable Lévy processes, the CGMY process is significant in finance because it provides a comprehensive framework for modelling the statistical properties of asset returns. Unlike traditional Gaussian models, the CGMY process can accommodate both frequent small moves and rare large jumps. The ability to capture the fine structure of asset returns, including skewness and kurtosis, allows for more accurate pricing of derivatives and better risk assessment (Carr et al. 2002).

The CGMY process $X(t; C, G, M, Y)$ is defined by its Lévy density

$$k_{CGMY}(x) = \begin{cases} \frac{C\exp(-G|x|)}{|x|^{1+Y}} & \text{for } x < 0, \\ \frac{C\exp(-Mx)}{x^{1+Y}} & \text{for } x > 0 \end{cases} \tag{24}$$

Here, C is the activity level of the process ($C > 0$), G is the rate of exponential decay for negative jumps ($G \geq 0$), M is the rate of exponential decay for positive jumps ($M \geq 0$), and Y is the tail index controlling the heaviness of tails ($0 < Y < 2$).

The CGMY process extends the VG model by adding the parameter Y, which allows for more flexible modelling of the jump activity and variation. This additional parameter enables the CGMY model to capture both finite and infinite activity and variation, providing a richer structure for modelling asset returns (Carr et al. 2002). The characteristic function $\phi_X(u;t)$ of the CGMY process $X(t; C, G, M, Y)$ is given by

$$\phi_X(u;t) = \exp\left(tC\Gamma(-Y)\left[(M-iu)^Y - M^Y + (G+iu)^Y - G^Y\right]\right) \tag{25}$$

The CGMY asset price process is described by the following equation

$$S_t = S_0 e^{X_{t,CGMY}} \tag{26}$$

where $X_{t,CGMY}$ is the CGMY log-asset price process (Oosterlee and Grzelak 2019). The characteristic exponent for the CGMY log-asset price can be found in closed form as

$$\begin{aligned} \varphi_{\log S_t}(u) &= e^{iu\log S_0}\mathbb{E}\left[e^{iuX_{t,CGMY}} \mid \mathcal{F}(0)\right] \\ &= \exp\left[iu\left(\frac{1}{t}\log S_0 + r + \omega - \frac{1}{2}\sigma^2\right)t - \frac{1}{2}\sigma^2 u^2 t\right] \times \phi_X(u;t) \end{aligned} \tag{27}$$

where ω is the drift correction term given by

$$\omega = -\frac{1}{t}\log\left(\phi_X(-i)\right) \tag{28}$$

This modification in the characteristic function is necessary to ensure the process adheres to the risk-neutral dynamics under the EMM, making the discounted process a martingale (Oosterlee and Grzelak 2019).

3 Analytical Framework

This section details the methodology employed to model and analyze the pricing of short-dated options, specifically focusing on 1DTE SPX options. The approach encompasses numerical technique employed, model calibration and implied density, each of which is discussed in the subsequent sections.

3.1 COS Fourier Transform

Building on the examination of the characteristic functions of the models, which allow us to handle various underlying dynamics effectively, this paper utilises the COS Fourier numerical method. The COS method by Fang and Oosterlee (2009), is a novel option pricing method based on Fourier-cosine series expansions.

The COS method is based on the Fourier-cosine series expansion of the density function. For a function $f(x)$ that represents the Fourier-cosine series expansion supported on an interval $[a, b]$

$$f_x \approx \sum_{k=0}^{N-1} V_k \cos\left(\frac{k\pi(x-a)}{b-a}\right) \tag{29}$$

where the coefficients V_k are defined as

$$V_k = \frac{2}{b-a}\int_a^b f(x)\cos\left(\frac{k\pi(x-a)}{b-a}\right)dx \tag{30}$$

The COS method is applied to options pricing by expressing the risk-neutral valuation formula in terms of the Fourier-cosine series expansion. The option value C_0 at the initial time t_0 is given by

$$C_0 = e^{-r(T-t)}\sum_{k=0}^{N-1}\mathrm{Re}\left(e^{ik\pi(\ln(S_0/K)-a)/(b-a)}\phi_X\left(\frac{k\pi}{b-a}\right)\right)V_k \tag{31}$$

where $\phi(\cdot)$ is the characteristic function of the underlying price process, and V_k are the Fourier-cosine coefficients of the option payoff function.

A wide truncation range is necessary to ensure accurate pricing and calibration for 1DTE options, where the sensitivity to distributional features is especially pronounced, thus a trucation range of 20 has been employed across the entire study, since narrow truncation can lead to oscillatory errors (Gibbs phenomenon), distorting option prices. A wider range helps mitigate these errors, leading to smoother and more accurate pricing especially when trying to capture the heavy tails of the underlying distribution.

The COS method has several key features. Firstly, it exhibits exponential convergence for smooth density functions, which significantly enhances computational efficiency.

Secondly, the COS method's computational complexity is proportional to the number of terms in the Fourier-cosine expansion, making it advantageous for high-dimensional problem-solving. Additionally, the method is versatile, capable of accommodating various underlying dynamics, such as Lévy processes and the Heston stochastic volatility model. Finally, the COS method provides a highly efficient approach for retrieving the density function from the characteristic function, which is crucial for calibration.

While the COS method is highly efficient and flexible, it does have some drawbacks, which are discussed in detail in the original paper by Fang and Oosterlee (2009). These include potential challenges in handling very complex payoffs and the need for careful selection of truncation intervals for the Fourier-cosine series expansion. Building upon the efficiency of the COS method, the next critical step in our analysis is the calibration of the model parameters to observed market data.

3.2 Model Calibration

With the data properly prepared, the next step involves model calibration, a critical process in financial modelling where the parameters of a model are adjusted so that the model's output matches observed market data. This process is particularly challenging for options pricing models due to the ill-posed nature of the calibration problem (Cont 2010). The calibration problem can be framed as an inverse problem where one seeks to infer model parameters from observed market prices, ensuring that the model accurately prices a set of liquidly traded options.

The calibration process primarily focuses on minimizing a loss function with respect to the parameter set Θ. The choice of loss function, or objective function, is crucial, and selecting the appropriate one for the problem at hand is an important task. While many objective functions are commonly used in empirical research, they often have limitations when calibrating models for short-maturity options, such as 0DTE options. For instance, the Root Mean Squared Error (RMSE) loss function, as given below, are widely employed

$$\min_{\Theta} \text{RMSE} = \sqrt{\frac{1}{N_K}\sum_{j=1}^{N_K}\left(\frac{C^{\text{Mkt}}(K_j,T)-C^{\text{Mod}}(K_j,\Theta)}{BS_{t,K}^{\text{vega}}}\right)^2}. \tag{32}$$

where N_K is the number of unique strikes for a specific DTE options quoted at the same time and $BS_{t,K}^{\text{vega}}$ is the Black-Scholes vega as follows

$$\begin{aligned} BS_{t,K}^{\text{vega}} &= S_0\sqrt{T}N'(d_1), \\ d_1 &= \frac{\ln\left(\frac{S_0}{K}\right)+\left(r+\frac{\sigma^2}{2}\right)T}{\sigma\sqrt{T}}. \end{aligned} \tag{33}$$

Accurately pricing deep OTM options is critical in this research, as these options are more sensitive to model specifications and often exhibit more pronounced deviations from observed market prices. Hence, the weighted RMSE objective function above effectively accounts for the sensitivity of option prices to changes in volatility, which is particularly important for deep OTM options. By weighting the errors with the Black-Scholes vega, the calibration process prioritizes minimizing errors where the model is most sensitive, leading to more accurate pricing for OTM short-maturity options. This approach not only addresses the limitations of traditional loss functions but also ensures a more robust calibration outcome for options that are often the most challenging to price accurately.

Alternatively, the Mean Squared Error of the Implied Volatilities (IVMSE) captures the nuances of these options better

$$\min_{\Theta} \text{IVMSE} = \frac{1}{N_K} \sum_{j=1}^{N_K} \left(iVol^{\text{Mkt}}(K_j, T) - iVol^{\text{Mod}}(K_j, \Theta) \right)^2 \tag{34}$$

While the IVMSE objective function is more suited to capturing the volatility surface, it poses significant computational challenges, particularly in terms of time efficiency. Computing the Black-Scholes implied volatility after obtaining the model prices adds another layer of complexity and introduces an additional optimization routine where one must loop through different strikes.

While this research primarily employs non-linear least squares for model calibration using the *lsqnonlin* MATLAB function, it is important to acknowledge the potential impact of parameter uncertainty on the accuracy of the pricing models, particularly in the context of short-dated options. Small deviations in parameters can lead to significant pricing and hedging errors, especially for options with very short maturities, such as 1DTE options.

Non-linear least squares is a widely used technique for model calibration, but like any method, it assumes that the estimated parameters are the most likely values given the data. However, this approach does not explicitly account for the uncertainty in these parameter estimates. As a result, the calibrated model might be sensitive to small changes in the input data, which could lead to inaccuracies in the pricing and hedging of short-dated options.

Moreover, the `lsqnonlin` method only finds a local minimum rather than a global minimum. This means that the minimization of the objective function is highly dependent on the initial guesses for the parameters. If the initial guesses are not close to the true parameter values, the calibration may converge to a suboptimal solution, leading to less accurate pricing and hedging. This sensitivity to initial guesses is particularly challenging in models with many parameters, such as the two-factor Heston model.

To address this issue, for models like the two-factor Heston model, it is often necessary to use a global optimization technique, such as particle swarm optimization `PSO`, to obtain a good set of initial guesses. These initial guesses can then be refined using the `lsqnonlin` method to achieve a more accurate calibration. This procedure is adopted similarly from the work of Mrázek and Pospíšil (2017), where they first obtained initial guesses using a genetic algorithm, which were then refined by the non-linear least squares method. By combining these methods, they effectively balanced the exploration of the parameter space with the precision of local optimization, thereby improving the robustness and accuracy of the model calibration.

In future research, it would be beneficial to explore methods that incorporate parameter uncertainty directly into the calibration process. Approaches such as stochastic calibration or robust optimization could potentially enhance the reliability of the pricing models by providing a more comprehensive view of the risks associated with parameter estimation errors. These methods could offer a more resilient framework for pricing and hedging, particularly in the context of highly sensitive financial instruments like short-dated and exotic options.

3.3 Implied Density

Implied density is a powerful tool for extracting information from market prices, particularly for short-dated options where market expectations can change rapidly. Its application extends beyond pricing and risk management to areas such as stress testing and scenario analysis, offering a comprehensive view of the potential future states of the market. The concept of recovering the probability distribution from option prices was initially developed by Breeden and Litzenberger (2015), and later expanded upon by Jackwerth (1996), illustrating its practical applications in financial markets. The implied risk-neutral density (IRND) provides valuable insights into the anticipated price movements of the underlying asset within an extremely short time frame, which is of particular interest to traders and risk managers. The work of Ross (2015) provides further insights into the dynamics of implied density and its implications for market behavior.

The implied density is derived from the prices of European options and reflects the market's consensus on the probability distribution of the underlying asset at the option's expiration. This information is particularly useful for analyzing and predicting potential market behaviors, such as identifying the likelihood of extreme price movements (tail risk) or assessing the expected volatility around a key economic event.

Mathematically, the implied risk-neutral density $f_{RN}(K)$ is related to the second derivative of the European call option price with respect to the strike price K. The relationship can be expressed as

$$f_{RN}(K) = e^{rT} \frac{\partial^2 C(K)}{\partial K^2}, \tag{35}$$

where $C(K)$ is the call option price, r is the risk-free interest rate, and T is the time to maturity. This second derivative can be computed numerically using finite difference methods.

To approximate the second derivative using finite differences, the central difference method can be applied

$$\frac{\partial^2 C(K)}{\partial K^2} \approx \frac{C(K+h) - 2C(K) + C(K-h)}{h^2}, \tag{36}$$

where h is a small increment in the strike price. A similar approach is applied to put options, where the second-order derivative of the put price with respect to the strike price is approximated in the same manner. By applying this method across different strikes, the implied density function can be constructed, providing a continuous probability distribution for the underlying asset's price at expiration.

Moreover, an alternative method for obtaining the implied density involves the use of characteristic functions. The characteristic function is closely related to the implied density of the underlying asset, and the implied density can be obtained by taking the inverse Fourier transform of the characteristic function once the model is suitably calibrated

$$f(x) = \frac{1}{2\pi} \int_{-\infty}^{\infty} e^{-iux} \phi_X(u) du, \tag{37}$$

where $\phi_X(u)$ is the characteristic function of the log-price of the underlying asset. This method allows for a seamless transition between the characteristic function, option prices, and the implied probability distribution of the underlying asset.

4 Numerical Analysis

This section presents the empirical results of the study. It begins with a summary of the data preprocessing steps, followed by an evaluation of the calibration model's performance. Next, the in-sample and out-of-sample results are compared to assess the model's predictive accuracy. Finally, the implied density of the option models is analyzed and compared to market data.

4.1 Option Data

To understand the dynamics of short-maturity options, the research begins by analyzing 1DTE SPX options end-of-day data, extracted as of 30th March, 2023, from Optiondsdx for the 1 day calibration. The annual federal interest rate on this date was recorded at 5.00%, which was used as a key input in the analysis in the form of a continuously compounded rate.

The preprocessing of the data involved several steps to ensure its quality and relevance. Initially, observations were filtered to retain only those with a trading volume greater than 25, thereby focusing on actively traded options that provide meaningful insights. To avoid distortions in pricing, observations where the bid or ask prices were zero were removed, as such instances do not reflect active market conditions. Additionally, entries with negative bid-ask spreads, indicative of potential data errors, were eliminated.

Given that the last traded price might not accurately reflect the market's supply and demand dynamics, the mid-quote was computed to represent a fair value of the options. This value was calculated as the average of the bid and ask prices. The analysis focused on out-of-the-money (OTM) options, which are of particular interest for their speculative nature, leading to the exclusion of in-the-money (ITM) call and put options from the dataset. Observations where the mid-quote was identical across different strikes were filtered out to maintain the variability necessary for robust model calibration. Finally, care was taken to maintain the monotonicity of mid-quotes across both calls and puts, ensuring consistency in the option pricing structure.

To ensure a continuous dataset for further analysis, missing strike prices were interpolated using the spline method. This interpolation allowed for a more comprehensive examination of the option series. Furthermore, since the SPX options are option on futures the research computes the implied forward price to identify the at-the-money (ATM) strike, which is crucial for calibrating models to market conditions. The ATM strike was determined as the price where the difference between the call and put prices was closest to zero. This can be observed mathematically using the put-call parity as below

$$\begin{aligned} C + Ke^{-rT} &= P + S, \\ C - P &= S - Ke^{-rT}, \\ 0 &= e^{-rT}(F - K), \\ F &= K. \end{aligned} \tag{38}$$

4.2 1 Day Calibration

As shown in Table 1, among the jump models, the VGB model demonstrates superior performance, reflecting its flexibility in capturing skewness and kurtosis in the return distribution. These characteristics are particularly crucial for accurately modelling the tails

Model	RMSE	IVMSE
VG	2.6389	0.0018
NIG	4.5662	0.0022
CGMY	5.0740	0.0012
VGB	**1.0455**	**0.0001**
NIGB	1.5741	0.0002
CGMYB	2.4249	0.0005
Heston	2.6392	0.0030
Two-Heston	2.5232	0.0022

Table 1: Calibration Performance of 1DTE SPX Options

of the distribution where jumps are more pronounced. When comparing the pure jump Lévy models with their counterparts where the diffusion component via the Brownian motion is added, one can observe a noticeable improvement. This is due to the fact that skewness and excess kurtosis for Lévy processes are inversely proportional to time. Thus, for very short maturities, these statistics might increase rapidly. Adding the Brownian motion mitigates this issue as its presence increases the total variance of the process, but does not affect the third and fourth-order cumulants used to calculate skewness and excess kurtosis. This can be illustrated by the following equation:

$$\text{sk} = \frac{C_3(t)}{\sqrt{C_2(t)}} \frac{1}{\sqrt{t}} \tag{39}$$

where $C_2(t) = \sigma^2 + \text{Var}(Y_t)$ represents the second cumulant which includes the variance of the Brownian motion component σ^2. Here, $C_3(t)$ is the third cumulant. The addition of the Brownian motion increases $C_2(t)$, the denominator of the skewness equation, thereby reducing the skewness and making the model more capable of accurately capturing the smile of the implied volatility surface.

Within the pure jump models, one observes that the CGMY model performs better than the VG and NIG models because it provides more control over the jumps and their variation. The CGMY model's ability to adjust the frequency and severity of jumps allows for a better fit to the data, which is crucial for capturing the finer details of the return distribution, particularly the tails. However, when comparing the CGMY model with its diffusion counterpart (CGMYB), there is not as significant an improvement as observed with other models like VG to VGB or NIG to NIGB. This could be attributed to the fact that the CGMY model already provides a high degree of control over the jumps, and adding a Brownian motion component may not enhance its calibration performance as much. The CGMY model's inherent flexibility might already capture the essential dynamics that the Brownian motion aims to address, resulting in a less pronounced benefit when adding diffusion.

When comparing the jump diffusion models to the stochastic volatility models, a distinct pattern emerges where all of them consistently outperforms both the Heston and Two-Heston models. This observation highlights a critical limitation of the stochastic volatility models: their inability to fully capture the implied volatility smile, which is a

pronounced feature in short-maturity options markets. The Heston model, in particular, relies on a symmetric square-root process for variance, which may not accurately reflect the skewness or asymmetry driven by market participants' perception of risk and the probability of extreme events.

Furthermore, the Heston model's ability to capture the leverage effect—where negative asset returns lead to an increase in future volatility—is somewhat limited, especially in the context of short-dated options like the 1DTE ones analyzed here. While the leverage effect is typically a longer-term phenomenon, the volatility feedback effect—where an increase in volatility leads to a decrease in stock returns—can be more pronounced in the short term. The Heston model incorporates a correlation parameter ρ to account for the relationship between the asset price and its volatility, but this parameter may not fully capture the intensity and immediacy of the volatility feedback effect in very short time frames. In practice, the volatility feedback effect can have a more immediate impact on short maturities, causing the Heston model to fall short in reflecting the true dynamics of the market. This shortcoming contributes to its underperformance compared to jump diffusion models like VGB, which are better suited to capture the abrupt changes and asymmetries in volatility that are critical for accurately pricing 1DTE options.

In summary, while both RMSE and IVMSE generally align in assessing the relative performance of the models, highlighting NIG as the superior choice, a notable discrepancy arises in the case of the CGMY model. This inconsistency may stem from the RMSE approach, which, while computationally more efficient, serves as an approximation to the more precise IVMSE. Given this potential trade-off between efficiency and accuracy, the focus of further analysis in this study will shift towards the IVMSE objective function to ensure a more accurate evaluation of model performance.

Model	**Optimal Parameters (1 Day)**				
VGB	$\beta = 0.45$	$\theta = -0.1457$	$\eta = 0.001$	$\sigma = 0.1511$	
NIGB	$\alpha = 7.9911$	$\beta = -3.6891$	$\delta = 0.0763$	$\sigma = 0.1467$	
CGMYB	$C = 0.343$	$G = 5.9399$	$M = 5.472$	$Y = 0.01$	$\sigma = 0.1467$
Heston	$\kappa = 3.7001$	$\theta = 1.5996$	$\eta = 9.9051$	$\rho = -0.5648$	$v0 = 0.0256$
Two-Heston	$\kappa_1 = 0.8194$	$\theta_1 = 4.2741$	$\eta_1 = 1.1941$	$\rho_1 = 0.99$	$v0_1 = 0.01$
	$\kappa_2 = 3.4614$	$\theta_2 = 0.01$	$\eta_2 = 10$	$\rho_2 = -0.99$	$v0_2 = 0.0188$

Table 2: Optimal Parameters from 1 Day Market Data Calibration

As demonstrated in Table 2, the values of the optimal model parameters across the VGB, NIGB, CGMYB, and Heston models align well with the expected sensitivities of these parameters, especially considering the highly volatile nature of short maturity options. Each parameter's calibration is consistent with its underlying role in capturing specific characteristics of the return distribution, such as skewness, kurtosis, and jump dynamics. For example, in the NIG model, the α parameter, which controls the tail heaviness and overall steepness of the density function, falls within the expected range for 1 DTE options, typically between 5 and 20. The calibrated α value reflects a lighter tail, which is appropriate given the market's conditions, indicating that the market is not experiencing extreme tail risks. Similarly, the β parameter, which determines the skewness of the distribution, shows a negative value, indicating the presence of left skewness,

consistent with the market's risk perception for short-term options. In the context of the NIG model, a negative β results in a distribution that is skewed to the left, reflecting the asymmetry often observed in the log returns of the underlying asset, such as the S&P 500 index. For underlying assets, particularly in highly liquid and broad market indices, negative skewness in log returns is common due to the market's tendency to react more sharply to negative news or downturns. The δ parameter, controlling the scale of the distribution, is small, typically expected to be within the range of 0.01 to 0.5 for short-dated options. This indicates a narrow distribution scale, suggesting a precise fit to the observed market volatility. These results suggest that despite the wide calibration bounds, the optimization process effectively found local minima that are well-justified based on the characteristics and sensitivities of each model's parameters. This is further supported by past research, which shows that these parameter ranges are typically expected for short-term, highly volatile options.

However, the Two-Heston model presents a distinct case, where several parameters, including the correlation coefficients and variance levels, are driven to their bounds during the calibration process. This phenomenon highlights a significant limitation of the two-factor Heston model when applied solely to short maturity options. The primary intent behind extending the Heston model to include a second stochastic volatility factor is to enhance its flexibility, allowing it to simultaneously fit both short-term and long-term options data. Yet, when the calibration focuses exclusively on short-term options, this added complexity may lead to overfitting or drive the parameters to extremes that are not easily interpretable. Specifically, the parameters that control the short-term and long-term volatility dynamics appear to be compensating for the lack of longer-term data, which would normally balance the model's calibration across different maturities. As a result, the optimal parameters for the Two-Heston model, in this context, are not entirely justified as they reflect the model's attempt to fit a single maturity while stretching the parameter bounds beyond what is typical or reasonable. This suggests that while the Two-Heston model is valuable for a broader spectrum of maturities, its application to short-term options alone may require additional constraints or modifications to avoid such calibration issues.

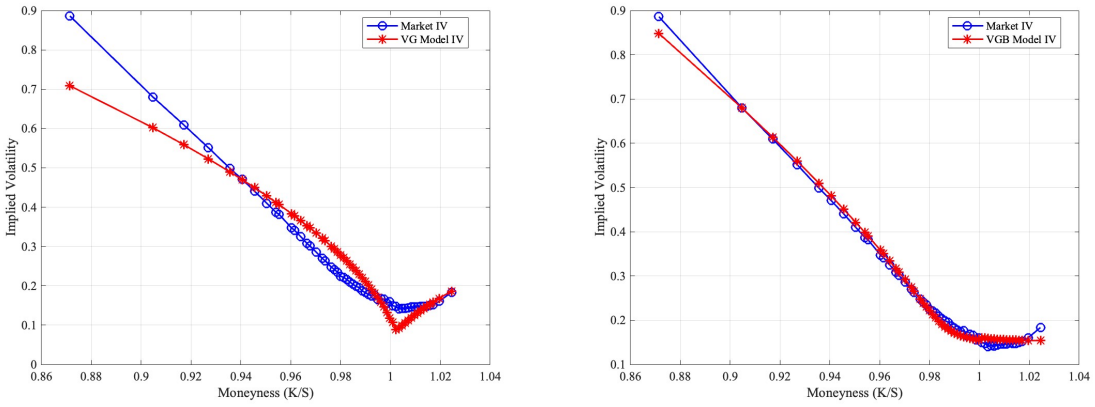

(a) VG Model (b) VGB Model

Figure 1: Implied Volatility Smile Comparison - Page 1

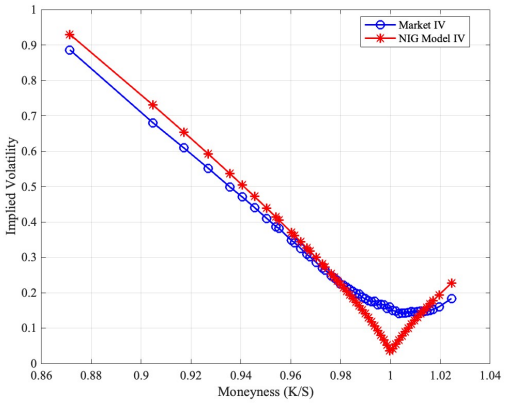

(c) NIG Model

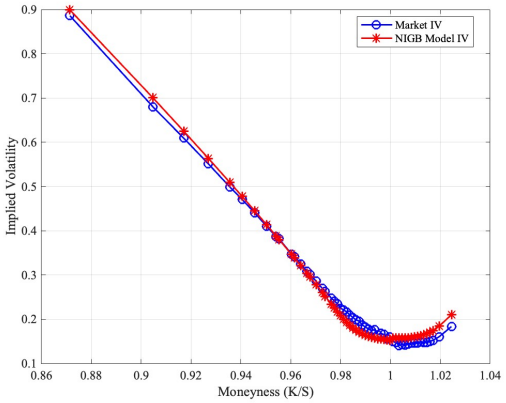

(d) NIGB Model

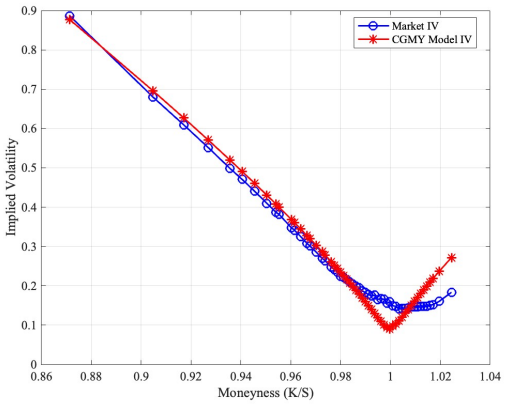

(e) CGMY Model

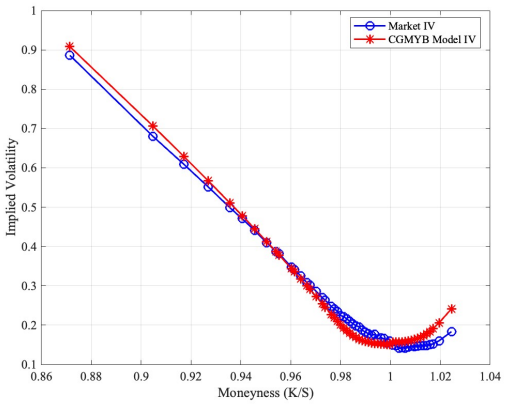

(f) CGMYB Model

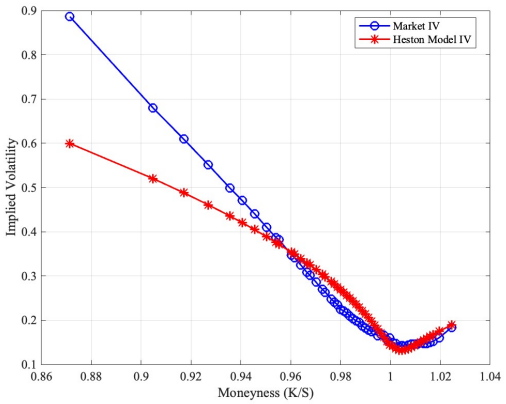

(g) Heston Model

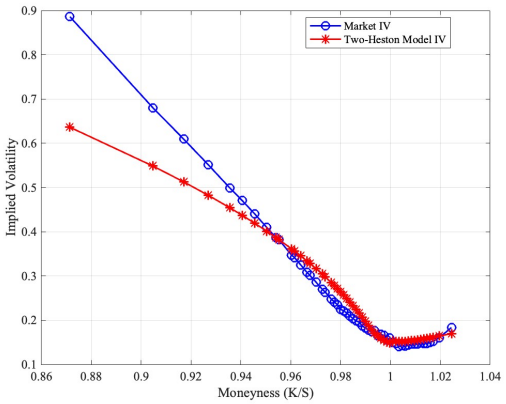

(h) Two-Heston Model

Figure 1: Implied Volatility Smile Comparison - Page 2

In the pure jump models, such as the VG, NIG, and CGMY models, a pronounced kink is observed at ATM strike. Also the implied volatilities for out-of-the-money (OTM) calls are overestimated, as seen in the right tail of the IV smiles for the NIG and CGMY. This overestimation arises from the nature of pure jump models, which inherently introduce higher skewness and kurtosis into the distribution, leading to a steeper and more pronounced volatility smile. In contrast, the jump diffusion models, including the VGB, NIGB, and CGMYB models, exhibit a much smoother IV smile. The inclusion of a diffusion component, allows these models to temper the higher-order moments such as

skewness and kurtosis. This additional diffusion helps to modulate the behavior of the tails of the distribution, leading to a better fit with the market data, particularly for OTM options.

Expanding on Figure 1, we observe that models like NIGB and CGMYB excel in capturing the steep rise in implied volatility associated with deep out-of-the-money (OTM) calls in Figure 1 which VGB fails to capture. More importantly, these models effectively reflect the market's sensitivity to extreme downside risks, significantly outperforming the Heston and Two-Heston stochastic volatility models in this region. Even the simple pure jump models offers improvement over the Heston models for deep OTM puts, its performance is substantially better, indicating that it almost fully captures the nuances of these extreme scenarios.

On the other hand, the Heston and Two-Heston models demonstrate their strength in modelling the volatility dynamics near at-the-money (ATM) options and the OTM calls on the right side of the smile. These models are well-suited to capturing the smoother, more gradual changes in implied volatility that are typical in these regions, where the market is less concerned with extreme movements and more focused on the central tendencies of the underlying asset's price behavior. The additional factor in the Two-Heston model further enhances its ability to reflect these dynamics, making it particularly effective for options near ATM and right-side OTM calls.

To gain deeper insight into how these models perform across different moneyness buckets, we will conduct both in-sample and out-of-sample analyses in the next section, which will allow us to further evaluate their effectiveness under market conditions which vary overtime.

4.3 In-Sample and Out-of-Sample

Following the insights gathered so far, we now turn our attention to the in-sample and out-of-sample performance of the models. The in-sample data covers the period from April 10th to April 13th, 2023, while the out-of-sample data spans from April 17th to April 20th, 2023. The analysis was conducted by first calibrating each model to the in-sample data to obtain the optimal parameters. These optimal parameters were then used to evaluate the models' performance out-of-sample, particularly focusing on options with high liquidity and trading volume during those dates. This approach is crucial for understanding how well each model fits the data used for calibration and, more importantly, how effectively they generalize to new, unseen data, thereby providing a comprehensive view of their robustness across different segments of the implied volatility smile.

Model	**In Sample**					**Out of Sample**				
	Moneyness (K/S)					**Moneyness (K/S)**				
	< 0.975	$0.975 - 1$	$1 - 1.01$	> 1.01	**All**	< 0.975	$0.975 - 1$	$1 - 1.01$	> 1.01	**All**
VGB	0.0002325	**0.00057909**	**0.0014528**	0.0011529	0.00089069	0.00073586	**0.0021556**	0.0035591	0.0020364	0.00242498
NIGB	**0.000041812**	0.00058144	0.0014532	0.00091485	**0.00074276**	0.00020015	0.0021644	**0.0035548**	**0.0013234**	**0.00201063**
CGMYB	0.00045352	0.00058553	0.0014565	**0.00091308**	0.00085351	**0.0001908**	0.0021823	0.0035662	0.0013491	0.00209729
Heston	0.010444	0.00061266	0.0014616	0.0011685	0.00208512	0.023798	0.0023212	0.0036080	0.0022122	0.00365811
Two-Heston	0.002571	0.00072826	0.0014573	0.0011441	0.00140512	0.0066326	0.0023854	0.0036162	0.0017948	0.00349991

Table 3: In-Sample and Out-of-Sample Performance across Moneyness Buckets through IVMSE

Upon examining the performance of the models across different moneyness buckets, we observe some significant deviations from the initial findings derived from the one-day calibration. Initially, the VGB model was identified as the best performer based on the

one-day calibration. However, the extended one-week calibration period reveals a more complex picture, highlighting the strengths and limitations of each model under different market conditions.

For deep OTM puts, where $K/S < 0.975$, the NIGB model demonstrates the lowest IVMSE in-sample, indicating its ability to capture the steep increase in implied volatility associated with extreme downside risks during the calibration period. Interestingly, when evaluated out-of-sample, the CGMYB model takes the lead, suggesting that while NIGB is effective in the calibration phase, CGMYB is better at generalizing to new data, possibly due to its flexibility in modelling the tails of the distribution.

In the moneyness range $0.975 \leq K/S \leq 1.0$, the VGB model continues to show the best fit, both in-sample and out-of-sample. This consistency underscores VGB's robustness in capturing the implied volatility near the money, where the option prices are highly sensitive to changes in the underlying asset's price. The model's performance in this region suggests that its structural components are particularly well-suited for modelling the relatively stable and symmetric sections of the volatility surface.

When considering call options that are OTM $1.0 \leq K/S \leq 1.01$, the VGB model still exhibits the lowest IVMSE in-sample, reflecting its strong calibration within this bucket. However, out-of-sample, the NIGB model surpasses VGB, indicating that NIGB's flexible structure allows it to better adapt to changes in market conditions. This shift suggests that while VGB provides an excellent fit during calibration, it may be more sensitive to the specific conditions of the sample, leading to a less robust performance when applied out-of-sample.

For OTM calls, where $K/S > 1.01$, the CGMYB model performs best in-sample, capturing the implied volatility dynamics effectively within the calibration period. However, in the out-of-sample evaluation, the NIGB model emerges as the most accurate whereas VGB gets outperformed by the Two-Heston model as well. This discrepancy highlights a critical limitation of the VGB model, which consistently underestimates the implied volatilities of OTM calls. The VGB model's tendency towards conservative estimates, likely due to its handling of negative jumps, leads to this underestimation. In contrast, the NIGB model's ability to better capture the upward jumps in implied volatility makes it more effective out-of-sample, particularly in the tails of the distribution where market moves can be more extreme.

Overall, when we evaluate the models across all strikes, the NIGB model emerges as the most robust and accurate, both in-sample and out-of-sample. This finding contradicts the earlier conclusion drawn from the one-day calibration, where the VGB model was deemed superior. The NIGB model's consistent performance across the extended calibration period suggests that it offers a more reliable fit, particularly when the calibration is extended to encompass a longer time horizon. This result emphasizes the importance of testing models over different periods and market conditions to fully understand their strengths and limitations. While the VGB model excelled in the short-term calibration, its conservative bias limits its effectiveness over longer durations, whereas the NIGB model's adaptability and flexibility make it a more dependable choice for capturing the full complexity of the volatility surface in real-world applications.

4.4 Implied Density

In this analysis, implied densities were extracted from end-of-day data. Since only a single maturity slice was available, the analysis was confined to a 2D plot across different

strike prices rather than the usual 3D surface. The market's implied volatilities were first calculated using the actual grid of strikes. The calibrated models' implied volatilities for 30th March, 2023 were then used to compute the second-order derivatives of option prices with respect to strike prices, using the finite difference method. This approach enabled a comparison of implied densities between the market data and the models.

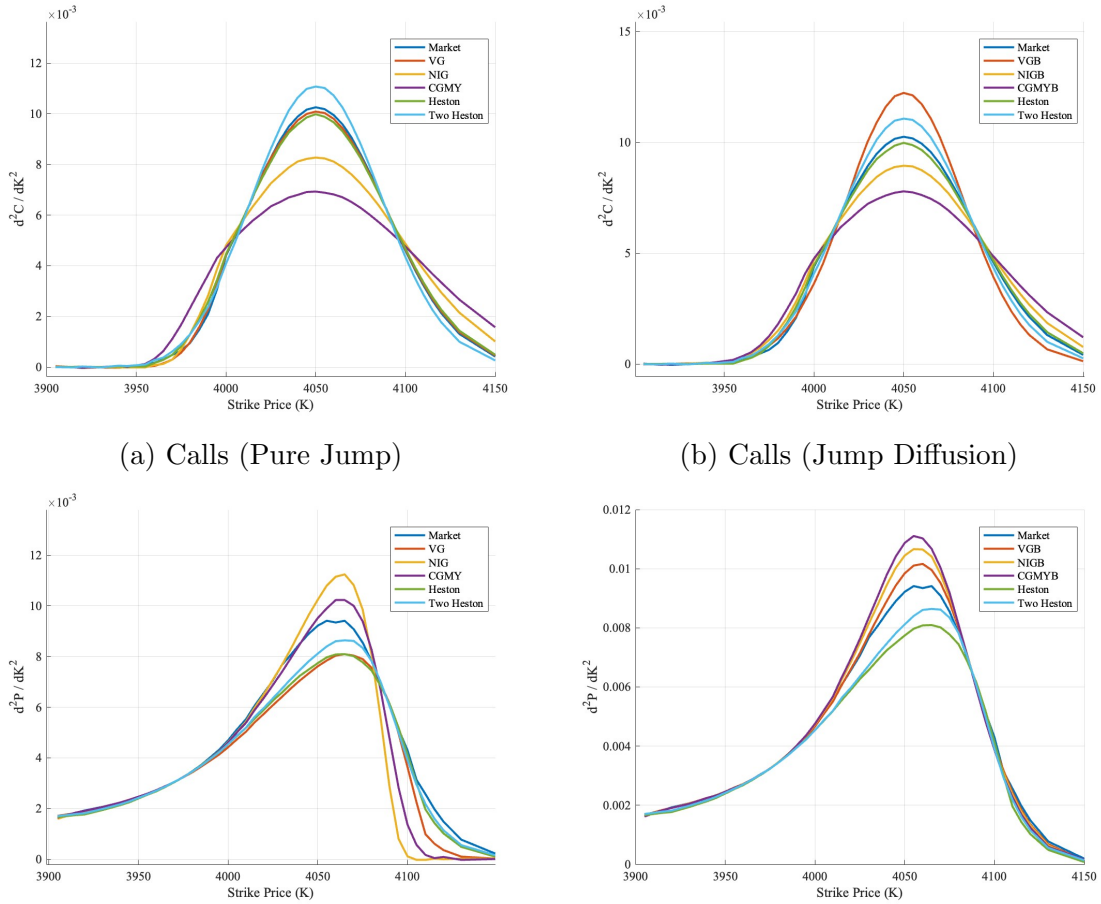

(a) Calls (Pure Jump)

(b) Calls (Jump Diffusion)

(c) Puts (Pure Jump)

(d) Puts (Jump Diffusion)

Figure 2: Implied Density Comparison between Market and Model for Calls and Puts.

In the pure jump setting, illustrated in Figure 2 panels (a) and (c) for calls and puts respectively, the VG and Two-Heston models demonstrate a strong alignment with the market-implied density, particularly in the tails. This indicates their robustness in capturing the probabilities of extreme price movements. For call options, the VG model nearly completely replicates the markets implied density but from panel (b) one can observe that its counterpart VGB fails to capture the nuances suggesting that introducing diffusion allows for a better implied volatility fit but not implied density. In the case of panel (b), the Heston model's performance is particularly surprising, given its typical characterization of stochastic volatility, which might not intuitively seem suited for short maturity options. This checks out with the specific conditions of the day under analysis—characterized by low volatility and a relatively stable SPX index (opening at 4046.74 and closing at 4050.83).

Similarly, for put options, the Two-Heston model stands out as the best fit for the market-implied density throughout, as depicted in panels (c) and (d). This model's success highlights the importance of accurately capturing the risk-neutral distribution

in environments where volatility changes are subtle and the price dynamics are more continuous than discrete. The relatively low volatility observed on the analysis day provides an intriguing context for evaluating the performance of different models. Pure jump and diffusion models, such as the NIG and CGMYB model, often emphasize the possibility of sudden large moves, which can introduce a bias towards fatter tails or higher peaks in the implied density. This might lead to a better fit to the implied volatility surface but results in a less accurate representation of the true implied density, which, under low volatility conditions, tends to be smoother and more centered around the mean.

In contrast, stochastic volatility models, including the Heston and Two-Heston models, appear to excel in such conditions. Their design inherently captures the continuous nature of price changes in a low volatility setting, producing a density that more accurately reflects the actual risk-neutral distribution of future prices. This suggests that in low volatility environments, where market conditions are more stable, the stochastic nature of volatility dominates over abrupt jumps, leading to a more faithful depiction of the underlying asset's price behavior.

The analysis of implied density for 1DTE options can offer several predictions. By examining the tails of the implied density, traders can gauge the probability of extreme price movements, which is essential for risk management, especially in markets with significant short-term uncertainties. Additionally, the shape and spread of the implied density function can provide insights into the expected volatility over the remaining life of the option. A wider implied density suggests higher expected volatility, which can inform trading strategies. The implied density also reflects the market's sentiment towards the underlying asset, such as the anticipation of sharp movements due to an impending economic event. For example, a bimodal distribution might indicate market uncertainty, with participants expecting a significant move in either direction.

5 Conclusion

The analysis presented in this thesis highlights the significant advantages of Lévy models in accurately capturing the nuances of short maturity options, particularly when compared to stochastic volatility models. Across both in-sample and out-of-sample tests, and regardless of moneyness segments, Lévy models with diffusion consistently deliver superior calibration performance. This robustness is especially pronounced in scenarios where the implied volatility smile exhibits steepness or asymmetry, areas where traditional stochastic volatility models, like the Heston model and its extensions, often struggle.

However, it is crucial to recognize the specific contexts in which the Heston model and its variants maintain utility. Notably, these models provide a better fit for the implied density when calibrated to periods characterized by low volatility. This suggests that while Lévy models excel in capturing more complex market dynamics, stochastic volatility models still hold value in specific market conditions, particularly in more stable environments where the volatility surface tends to be smoother and more symmetric.

Building on the findings of this research, several avenues for future exploration can be identified. One promising direction is the implementation of Sato processes, which represent an advancement over Lévy processes. As discussed in the literature review, Sato processes can potentially offer even more refined modelling of asset price dynamics, particularly in capturing the intricate features of financial markets that are not fully addressed by Lévy models. Another area worth investigating is the integration of stochastic

volatility models with jumps, such as the Bates model (2001) and its extensions like the Stochastic Volatility with Jumps (SVJ) model. These models combine the strengths of both stochastic volatility and jump dynamics, offering a more comprehensive framework for capturing the full range of market behaviors, especially during periods of sudden, extreme movements.

Moreover, one can extend the analysis to the 0DTEs data noting a few caveats. The time to maturity for 0DTEs is typically around 6 hours, which, when annualized, results in a very small value. This may lead to the numerical techniques in question to falter as the COS Fourier transform may struggle in converging and finding stable values for the 0DTE prices. Therefore, it's crucial to select a stable and reliable numerical scheme before delving into the implications for the options Greeks, particularly delta and gamma. In the case of 0DTEs, the standard Black-Scholes closed-form solutions may not yield values consistent with expected outcomes and thats where the numerical technique might provide some aid enabling the analysis for the delta and gamma hedging which is the main utility of 0DTEs.

The calibration process itself could benefit from further refinement. Future research could explore the adoption of advanced optimization algorithms designed to avoid local minima and achieve a global minimum more effectively. Additionally, extending the calibration to cover longer time horizons could provide insights into the temporal stability of model parameters and their predictive power over extended periods.

Finally, applying these models across different markets and asset classes could yield valuable insights into their generalizability and robustness. Such cross-market analysis could help identify universal principles that govern option pricing dynamics or highlight the need for market-specific adjustments to existing models.

In conclusion, although Lévy models have proven to be highly effective in several key areas of short-term option pricing, there remains considerable potential for further development and innovation within the broader field of financial modelling. By exploring the avenues suggested, future research can build on these models, ensuring their relevance and applicability in an ever-evolving financial environment.

Acknowledgements

I would like to express my deepest gratitude to my supervisor, Professor Laura Ballotta. Her unwavering support, insightful guidance, and invaluable expertise have been instrumental in the completion of this dissertation. Her encouragement and patience have inspired me to push beyond my limits, and her constructive feedback has significantly enhanced the quality of my work. It has been an honor to work under her supervision, and I am truly grateful for the opportunity to learn from such a distinguished mentor. I would also like to thank my family and friends for their constant encouragement and understanding, which has been a source of strength throughout this challenging and rewarding experience.

References

Albrecher, H., Mayer, P., Schoutens, W. and Tistaert, J. The Little Heston Trap. *Wilmott Journal*, pp.83-92. [online] Available at: https://perswww.kuleuven.be/~u0009713/HestonTrap.pdf [Accessed 26 Aug. 2024].

Bandi, F.M., Fusari, N. and Renò, R. (2023). 0DTE Option Pricing. ESSEC Business School Research Paper No. 2023-03, Johns Hopkins Carey Business School Research Paper No. 24-02. *SSRN Electronic Journal*. [online] Available at: https://ssrn.com/abstract=4503344 or http://dx.doi.org/10.2139/ssrn.4503344 [Accessed 26 Aug. 2024].

Barndorff-Nielsen, O.E. (1997). Normal Inverse Gaussian Distributions and Stochastic Volatility Modelling. *Scandinavian Journal of Statistics*, 24(1), pp.1–13. [online] Available at: doi:https://doi.org/10.1111/1467-9469.00045.

Black, F. and Scholes, M. (1973) The Pricing of Options and Corporate Liabilities. *Journal of Political Economy*, 8, pp.637-654. - References - Scientific Research Publishing. [online] Available at: https://www.scirp.org/reference/referencespapers?referenceid=1887191 [Accessed 26 Aug. 2024].

Breeden, D.T. and Litzenberger, R.H. (2015). Prices of State-Contingent Claims Implicit in Option Prices. *Journal of Business*, 51(4), 1978. [online] Available at: https://ssrn.com/abstract=2642349 [Accessed 26 Aug. 2024].

Carr, P., Geman, H., Madan, D.B. and Yor, M. (2002). The Fine Structure of Asset Returns: An Empirical Investigation. *The Journal of Business*, 75(2), pp.305–333. [online] Available at: doi:https://doi.org/10.1086/338705 [Accessed 26 Aug. 2024].

CBOE, 2023. The Rise of SPX & 0DTE Options. [online] Available at: https://go.cboe.com/l/77532/2023-07-27/ffc83khttps://go.cboe.com/l/77532/2023-07-27/ffc83k [Accessed 26 Aug. 2024].

Christoffersen, P., Heston, S.L. and Jacobs, K. (2009). The Shape and Term Structure of the Index Option Smirk: Why Multifactor Stochastic Volatility Models Work so Well. *Social Science Research Network*. [online] Available at: doi:https://doi.org/10.2139/ssrn.961037 [Accessed 26 Aug. 2024].

Cont, R. (2010). Model Calibration. *Encyclopedia of Quantitative Finance*. [online] Available at: doi:https://doi.org/10.1002/9780470061602.eqf08002 [Accessed 26 Aug. 2024].

Eberlein, E. and Madan, D.B. (2007). Sato Processes and the Valuation of Structured Products. *Quantitative Finance*, 9(1), pp.27-42, [online] Available at: doi:https://doi.org/10.2139/ssrn.957167 [Accessed 26 Aug. 2024].

Fang, F. and Oosterlee, C.W. (2009). A Novel Pricing Method for European Options Based on Fourier-Cosine Series Expansions. *SIAM Journal on Scientific Computing*, 31(2), pp.826–848. [online] Available at: doi:https://doi.org/10.1137/080718061 [Accessed 26 Aug. 2024].

Gatheral, J., 2011. The Volatility Surface: A Practitioner's Guide. *Hoboken: John Wiley & Sons*. [online] Available at: http://www.hk.free.fr/Docs/The%20Volatility%20Surface%20-%20A%20Practitioner's%20Guide%20%5BJim%20Gatheral%5D.pdf [Accessed 26 Aug. 2024].

Heston, S.L. (1993). A Closed-Form Solution for Options with Stochastic Volatility with Applications to Bond and Currency Options. *Review of Financial Studies*, 6(2), pp.327–343. [online] Available at: doi:https://doi.org/10.1093/rfs/6.2.327 [Accessed 26 Aug. 2024].

Jackwerth, J.C. (1996). Recovering Risk Aversion from Option Prices and Realized Returns. *SSRN Electronic Journal*. [online] Available at: doi:https://doi.org/10.2139/ssrn.7745 [Accessed 26 Aug. 2024].

Madan, D.B., Carr, P.P. and Chang, E.C. (1998). The Variance Gamma Process and Option Pricing. *Review of Finance*, 2(1), pp.79–105. [online] Available at: doi:https://doi.org/10.1023/a:1009703431535 [Accessed 26 Aug. 2024].

Mrázek, M. and Pospíšil, J. (2017). Calibration and simulation of Heston model. *Open Mathematics*, 15(1), pp.679–704. [online] Available at: https://eudml.org/doc/288332 [Accessed 26 Aug. 2024].

Oosterlee, C.W. and Grzelak, L.A. (2019). Mathematical Modeling and Computation in Finance. *WORLD SCIENTIFIC (EUROPE) eBooks*. [online] Available at: doi:https://doi.org/10.1142/q0236 [Accessed 26 Aug. 2024].

Ross, S. (2015). The Recovery Theorem. *The Journal of Finance*, 70(2), pp.615–648. [online] Available at: doi:https://doi.org/10.1111/jofi.12092 [Accessed 26 Aug. 2024].

Tankov, P. (2003). Financial Modelling with Jump Processes. *CRC Press*. [online] Available at: https://citeseerx.ist.psu.edu/document?repid=rep1&type=pdf&doi=708d0c3da79185805008d59f2f920dc5ea7e66fd [Accessed 26 Aug. 2024].